Stony Brook University

Analysis of Great Basin GPS transients

A Thesis Presented

by

Huiyu Yang

to

The Graduate School

in Partial Fulfillment of the

Requirements

for the Degree of

Master of Science

in

Geosciences

Stony Brook University

May 2014

Stony Brook University

The Graduate School

Huiyu Yang

We, the thesis committee for the above candidate for the

Master of Science degree, hereby recommend

acceptance of this thesis.

William Holt – Thesis Advisor
Professor, Department of Geosciences

Troy Rasbury – Second Reader
Professor, Department of Geosciences

Gary Hemming – Third Reader
Affiliated Associate Professor, Department of Geosciences

This thesis is accepted by the Graduate School

Charles Taber

Dean of the Graduate School

Analysis of Great Basin GPS transients

by

Huiyu Yang

Master of Science

in

Geosciences Program

Stony Brook University

2014

Abstract

The Great Basin of the western United States is one of the research hotspots in recent years because of its mysterious and complicated geologic and geophysical characteristics. There are several hypotheses that describe the active deformation and its association with lithospheric structure and mantle processes. The EarthScope program provides a large data set of geodetic information for understanding the active deformation processes there. In this thesis, using geodetic data provided by PBO program (which is an important part of EarthScope program), I analyzed continuous GPS time series to investigate possible transient deformation behavior within the Great Basin region. I analyzed time series between the time period of 2004.20 to 2011.20. Using this data, I generated time-dependent displacement and strain solutions for the whole region in 0.1 year time steps. Small, but spatially correlated, anomalous transient

movements of ~2mm are observed over several time periods. Several hypotheses can be applied to explain the behavior of the GPS stations, including possible movement along an active megadetachment [Wernicke et al., 2008], coupling with mantle flow driven by a lithospheric drip [West et al., 2009], or toroidal mantle flow through the western U.S. slab window [Zandt et al., 2008], and even the influence of variable hydrologic loading [G. Heki, 2013].

Contents

Figure contents

Introduction

In 2001, the U.S. National Science Foundation (NSF), the U.S. Geological Survey (USGS) and the U.S. National Aeronautics and Space Administration (NASA) have jointly launched a new ground-breaking science program in Earth exploration: The EarthScope program.

The Plate Boundary Observatory (PBO) is one part of the Earthscope program. It provides a precision geodetic instrument system, including more than 1000 GPS stations, spacing 100-200km, making a network extending from the Pacific coast to the eastern edge of the Rocky Mountains, from Alaska to Mexico [Williams *et al*.,2010] (fig.1). With this program, it is possible to gain uninterrupted position and strain measurement data at almost all times in western North America continent. Also, detection of crustal strain and GPS displacement transients provide a way to reveal the dynamic characteristics of the North American continent.

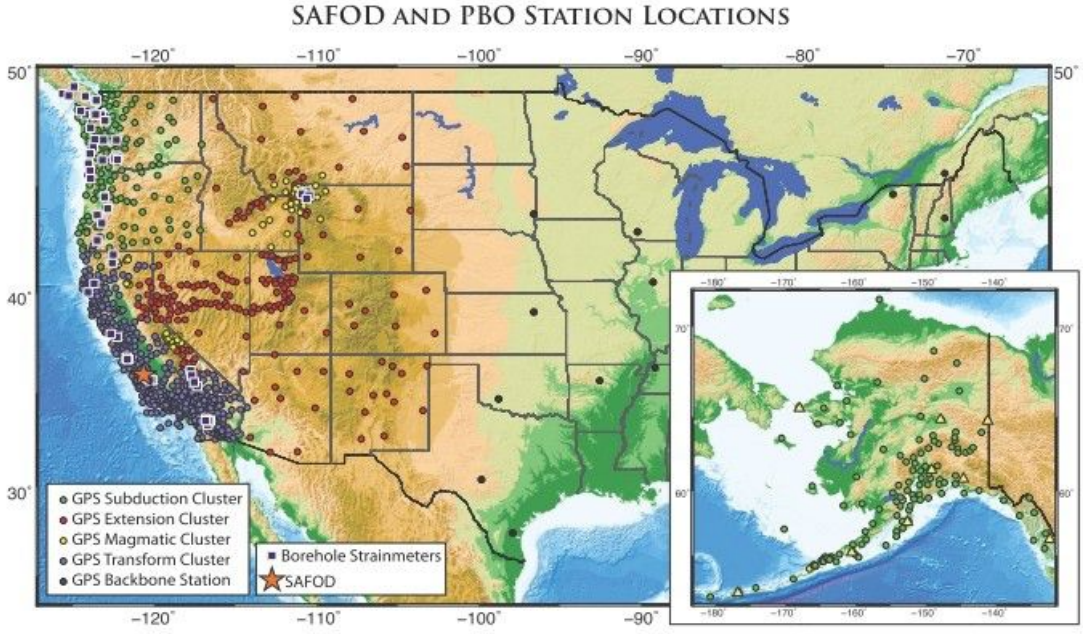

Fig. 1 Map of PBO stations [Williams *et al*.,2010]

The Great Basin is one region that attracts a lot of attention in Geological and Geophysical research. The Great Basin is in the western area of North America, where Basin and Range tectonics is wide spread. The tectonics belongs to Cordilleran belt. In this area, the Basin and Range is formed by extension [McCaffrey et al., 2007], and normal faults with lower dep angles are wide spread [Wernicke, 1981].

However, the structure of Great Basin is far more complicated. In 2010, Wernicke *et al*. [2008] found some regionally coherent transient velocity anomalies by analyzing the geodetic data from PBO program [Wernicke et al., 2010] (fig. 2).

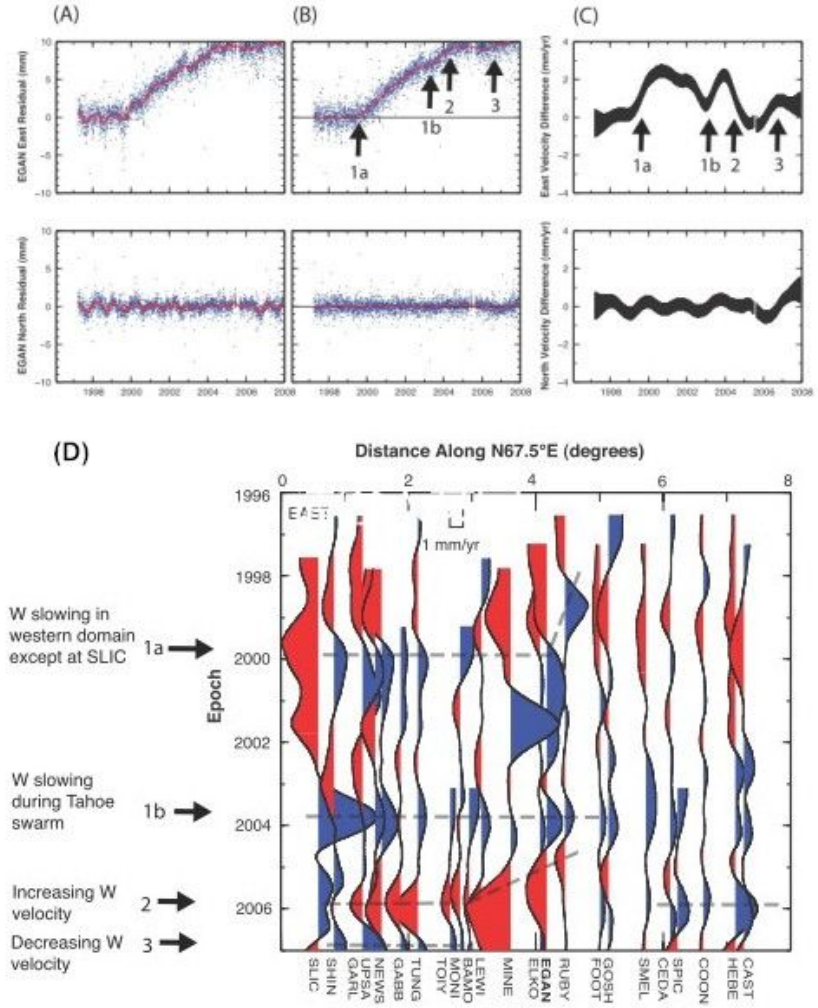

Fig. 2 (A) Unfiltered Time series of east and north components of position of site EGAN, relative to its average position prior to 2000.0. (B) Same with (A), but seasonal signals are removed. (C) Velocity time series derived from (B). (D) East-West velocity "geodogram" for all BARGEN sites. The site positions are projected onto N67.5^{0}E. Blue is to

These transient anomalies remain enigmatic and my research focus is to investigate PBO GPS data during 2004 – 2011. My goal is to determine if such transients continue to occur and characterize their spatial and temporal extent and magnitudes. Several physical mechanisms may possibly explain the transient behavior (described below) and I will investigate these as possible sources for crustal transient behavior.

(1) A lithospheric drip beneath Great Basin

Recent observations using seismograph arrays (USArray from EarthScope) by West *et al*. [2009] (Fig. 3) have revealed fast wave anomaly in the upper mantle, where volcanism is infrequent and thermal flux is lower. The central area of the Great Basin displays a local high-velocity that extends into the mantle as deep as 800 km depth [West *et al*., 2009]. Alternatively, this anomaly may represent ancient subducted Farallon Slab [Schmandt *et al.*, 2011].

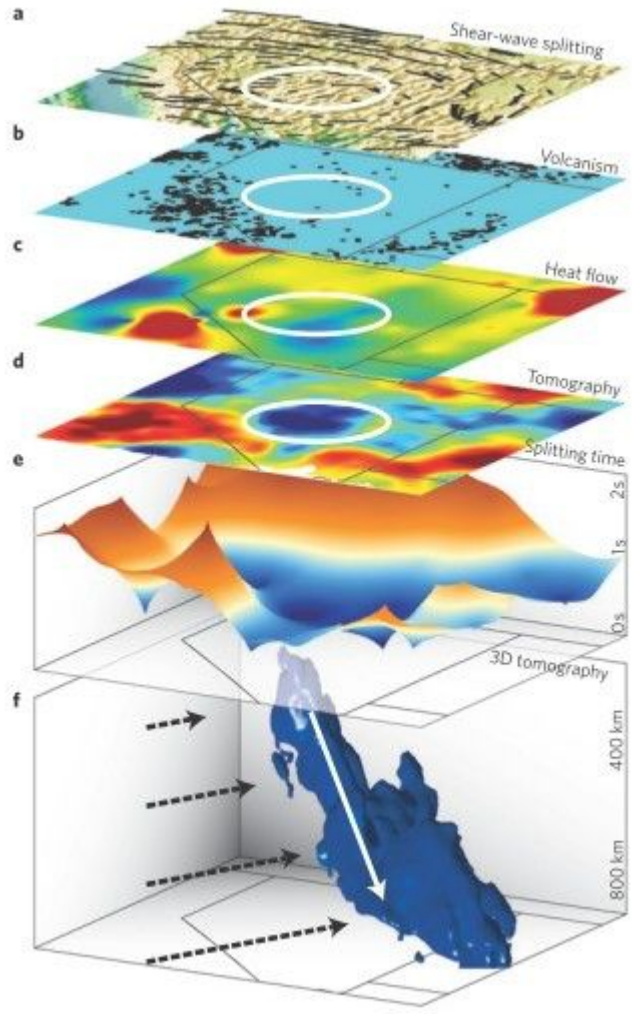

Fig. 3 "Drip" beneath the central Great Basin and other characteristics. a, Shear-wave splitting shows a circular pattern. b, Post-10-Myr volcanism (black circles) is more infrequent in this area. c, Heat flow showing reduced values (blue is around 50mWm^{-2}; yellow and red are more than 100mWm^{-2}). d, The horizontal slice at 200km depth of seismic tomography. e, Shear-wave splitting times surface showing the strong drop in the centre of Great Basin. f, 3-D tomography structure of the drip.
[West et al., 2009]

The mantle anomaly beneath the central Great Basin may produce mantle flow that acts on the overlying lithosphere by imposing tractions. The driving flow, or tractions, may be responsible for some of the forces that give rise to transient crustal strain anomalies.

(2) Toroidal mantle flow through the western U.S. slab window

For quite a long time, it has been known that the characteristics of southwest boundary in North America are the broader deformation band stretching from Pacific Ocean to Rocky Mountains. In the western part of the North American continent, it is observed that anisotropic fast-axis orientations of split SKS arrivals show as a circular pattern (Figure 3). Zandt *et al*. [2008] came up with a model that argued that this anisotropy was caused by toroidal mantle flow associated with Gorda–Juan de Fuca plate subduction from Mendocino

triple junction to the area beneath central Nevada. The position of this subducted slab can be obtained from seismic images and kinematic reconstructions [Zandt *et al*., 2008]. There is an enlarging triangular slab window [Dickinson *et al*., 1979], or slab-free gap [Severinghaus *et al*., 1990] on the northern edge of subducted Gorda-Juan de Fuca slab. Zandt's model argues for a strong toroidal mantle flow from beneath the slab to make a circular path, which is caused by the slab window. The influence of this mantle flow may couple to the overlying lithosphere and may influence crustal transient behavior.

(3) Possible movement along an active megadetachment

By analyzing geodetic data in Great Basin, Wernicke *et al*. [2008] saw a specific behavior in crustal transient motions between the eastern and western parts, which kept shifting between extension and contraction. Wernicke *et al*. proposed a model of a megadetachment along the base of the crust. When the megadetachment was locked, horizontal extensional strain accumulated in the upper part, which is the crust. Release of slip of the megadetachment resulted in reversal of motions in the upper crust, observed in the transients [B. Wernicke, 2008] (Fig.4).

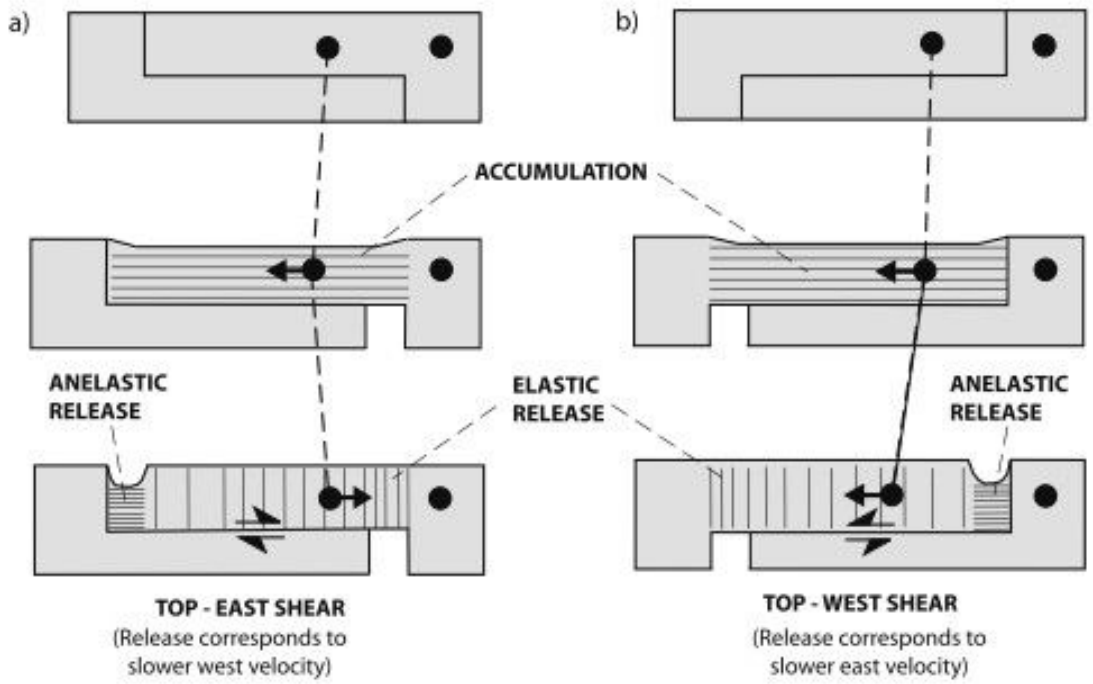

Fig. 4 Two possible strain release modes for the megadetachment along east-west (not to scale). (a) Strain release top-to-the-east. (b) strain release top-to-the-west. Black lines indicate direction of maximum elongation direction, with strain roughly proportional to spacing. [B. Wernicke, 2008]

(4) The influence of variable hydrologic loading

Climate change, or weather patterns from year-to-year, can lead to deformation of the ground surface, especially from the effects of hydrologic loading. Precipitation varies with seasons, while influences from rainfall, snow loading, and soil moisture can produce variable changes in pressures acting on the crust. In Japan, even the activity of earthquakes can be influenced by seasonal variations [M. Ohtake *et al*., 1999]. K. Heki, in 2013 evaluated multiple sources that might result in GPS transients, and found that snow, weighing over 1000kg per square meter in parts of Japan, is the largest factor affecting crustal motion changes [G. Heki, 2013] (Fig. 5).

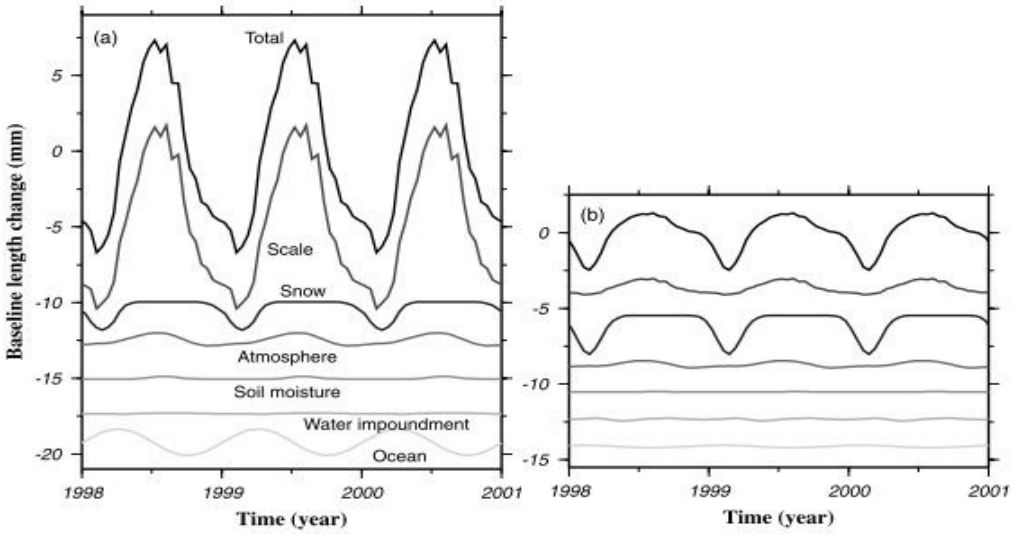

Fig. 5, Seasonal Baseline length changes according to various kinds of loads in (a) Kitami-Ibusuki and (b) Oogata-Utsunomiya. Contributions from scale, snow, atmosphere, soil moisture, water impoundment and ocean are shown from top to bottom. [G. Heki, 2013]

In the Great Basin the seasonal loading of the Great Salt Lake can lead to a variation of loading signals in the Great Basin of ~1mm [Elosegui *et al*. 2003]. Furthermore, several millimeters of movement can be associated with atmospheric pressure loading and continental-scale hydrological loading in the Great Basin [G. Blewitt, 2009]. Another probability of the seasonal influence is the human factor. For example, drawing water from a well will change the pressure distribution leading to an elastic deformation response.

Methodology

In this thesis, I use continuous GPS (cGPS) data from PBO to determine time-dependent displacement and strain fields in the Great Basin. The selection of the proper GPS sites is the first step of this program. When checking the region of Great Basin on UNAVCO's (a non-profit university organization of geosciences researchers and professors) data archive interface, more than 100 stations are available. A decent GPS site should meet several requirements:

(1) The span of the raw GPS data should be wider than the time frame from the beginning of 2004 to the beginning of 2011;

(2) Too much noise should be avoided when checking the brief time series provided by UNAVCO;

(3) The stations with significant data gaps, wide fluctuations, or excessively unrealistic outliers should be avoided.

Using the above criterion, only 23 stations are chosen. The 4-character IDs of them are:

SHIN	SLID	GARL	UPSA	TUNG	BAMO	LEWI	MINE
TOIY	TONO	ELKO	RUBY	GOSH	EGAN	FOOT	CEDA
SMEL	COON	EOUT	CAST	SPIC	SHLD	NEWS	

The continuous GPS time series from these stations are interpolated to obtain estimates of time-dependent displacements, using the method of Holt and Shcherbenko [W. E. Holt and G. Shcherbenko, 2013]. The raw GPS data show fluctuations that reflect the effects of seasonal changes. A fourth-order formulation, with seasonal terms, is used to interpolate the time

series.

(1)

The seasonal signal is estimated and removed and then a moving average filter with a short time length window also is used to provide a smoothed fit curve. Then the average-fit curve of the raw data, the fourth order polynomial curve, and the moving average smooth curve were graphed (see appendix). These curves not only show the long-term tendency of the separate stations movement, but also illustrate their short-term behavior. (Fig. 6)

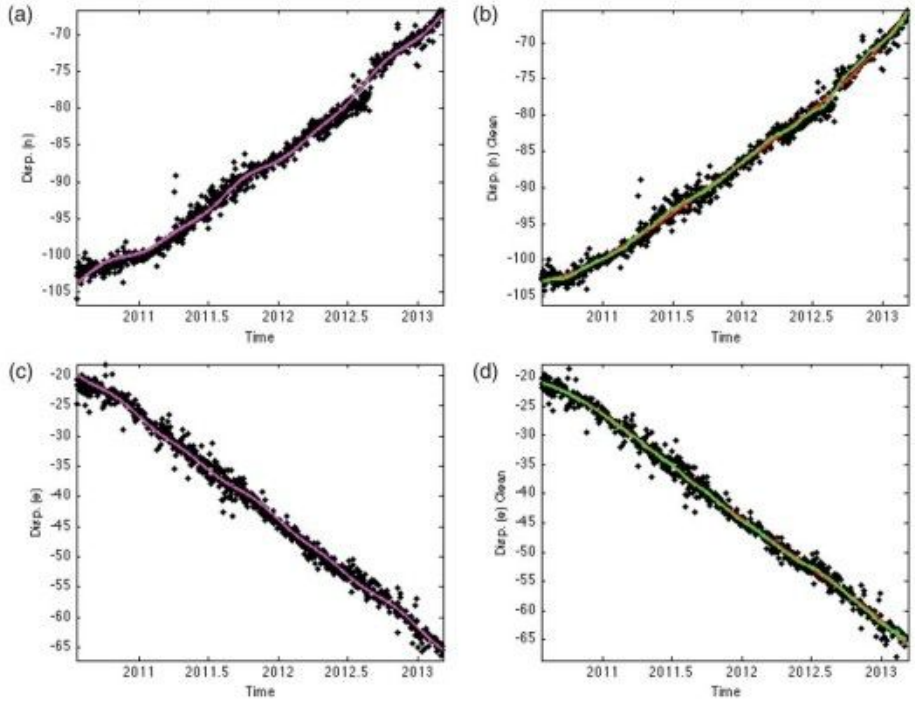

Fig. 6. Time-series analysis of the data from station P507. (a, b) Displacements along north–south direction. (c, d) Displacements along east – west direction. (a, c) magenta line fit to black dots, with the fourth-order polynomial fit; (b, d) green line fit to black dots, one-month moving average (centered) fit to residual time series (annual and semiannual terms removed), and red line, the fourth-order polynomial fit to the cleaned time series [W. E. Holt and G. Shcherbenko, 2013].

Displacements are output in time steps of 0.1y. Output from the 23 stations defines a time-dependent displacement field in this region.

Displacement fields are then fit with bi-cubic spline functions to obtain a continuous estimate of strain and displacement over time. The following functional is minimized in the fitting procedure

$$\chi = \sum_{cells\,ij,kl}\sum (\hat{e}_{ij} - e_{ij}^{obs})^T \mathbf{V}_{ij,kl}^{-1} (\hat{e}_{kl} - e_{kl}^{obs}) + \sum_{knots\,i,j}\sum (\hat{u}_i - u_i^{obs})^T \mathbf{V}_{i,j}^{-1} (\hat{u}_j - u_j^{obs}) \quad .$$

(2)

A reference field, obtained from time-averaged GPS observations in both of velocity and strain (Fig. 7, Fig. 8), is then removed from the time-dependent solution to provide a residual field [W. E. Holt and G. Shcherbenko, 2013].

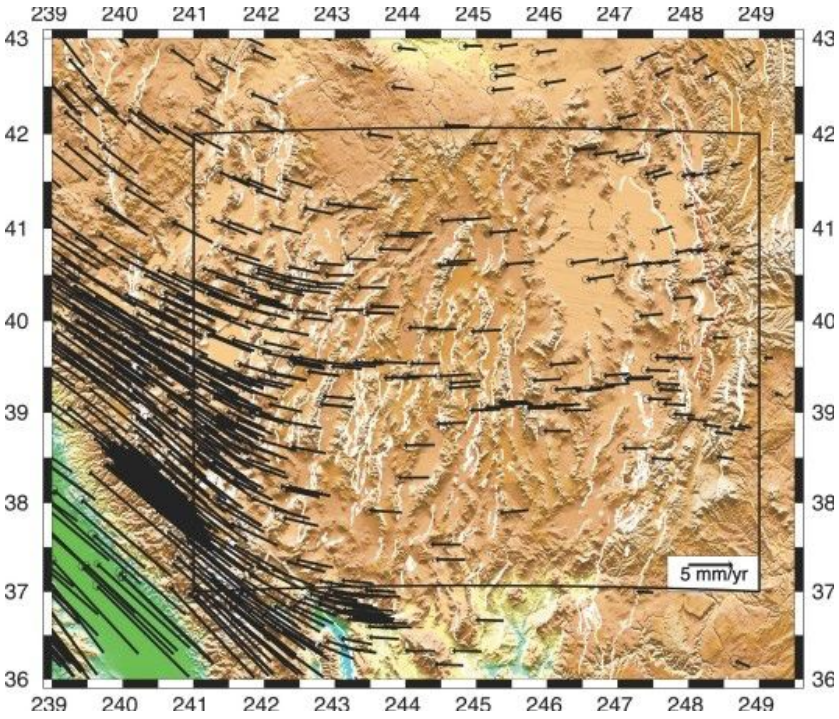

Fig. 7 velocity reference field, with motions relative to North America [W. E. Holt *et al.*in preparation].

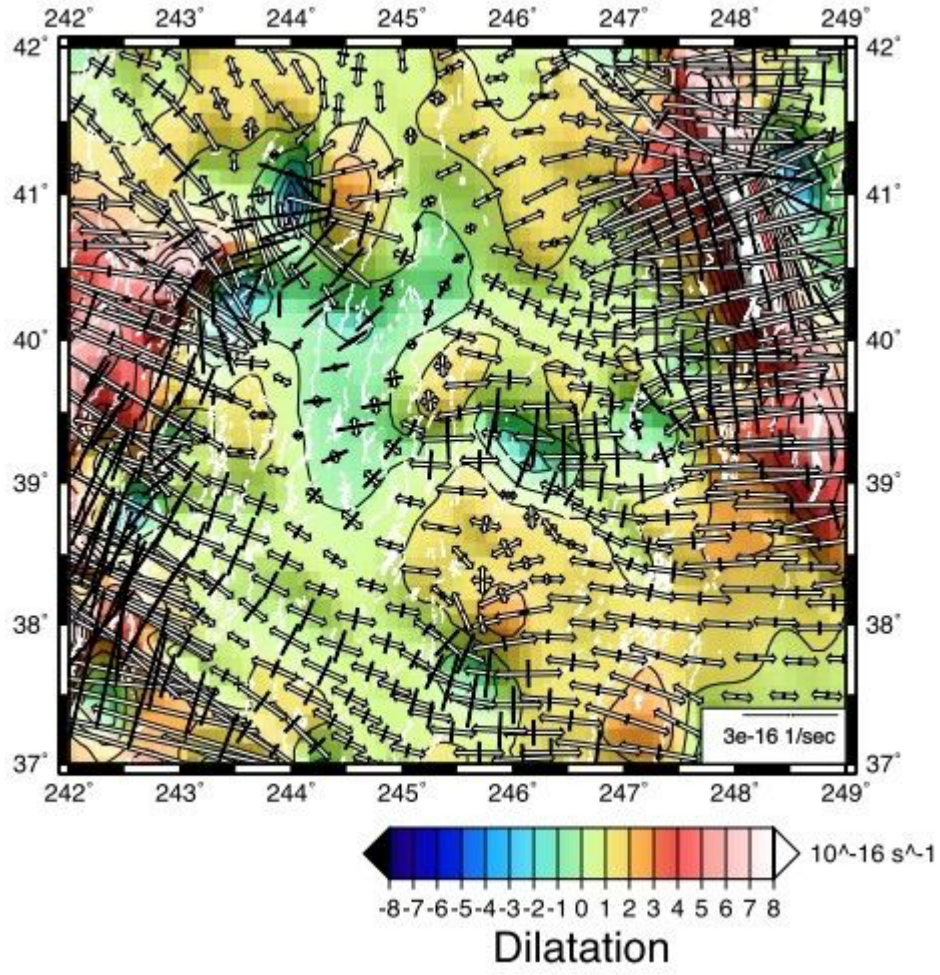

Fig. 8 Strain reference field with contours of dilatation strain rate and principal axes of strain rate (white vectors are extension, bold vectors are compression). [W. E. Holt *et al.*in preparation].

By subtracting out the reference field, the residual field is analyzed for significant departures from the reference solution. We found that the residual field contained a discrepancy that increases over time at all points. This discrepancy may be due to a difference between the GPS and the model reference frames. Because we are interested in the variations within the network, the average of the difference in the field was thus removed from that time-dependent GPS, so that all variations reflect only changes within the network, and not a difference between the reference frames of the observed GPS data and the reference field.

Results

The GPS time series of the stations often show significant variability, or wave-like patterns, such as station LEWI (Appendix). The residual field of displacements shows variations that periodically oscillate. In order to give a more clear impression the GPS transient behavior in Great Basin, the images of time-dependent displacement and strain fields in steps of 0.1 years are made into a short video, with the time period 2004.20 to 2011.20.

Observing the continuous changes of the images, the Great Basin area can be divided into an eastern region and a western region, where relatively distinct patterns of correlated movement and strain can be identified. Wernicke *et al*. [2008] also noted that the eastern and western Great Basin regions behaved differently.

(1) The Eastern Region

From 2004.20 to 2006.30, two distinct displacements to the east can be identified, being ~2mm from 2004.30 to 2004.50 and ~1.5mm from 2005.1 to 2005.30, respectively (Fig. 9). These are followed by a displacement to the northwest of ~2mm from 2005.60 to 2005.80 (Fig. 10) and a displacement to the east of ~2mm from 2006.0 to 2006.20.

The east region of the Great Basin remains relatively quiet, during 2006.40 to 2008.40, with very small displacement signals (Fig. 11).

From 2008.40 to 2009.00, the stations are move in the southeast direction with an average displacement of only ~1mm/y during this time interval (Fig. 12).

From 2009.50 to 2011.00, the stations are displaced toward the southeast direction again, with an average displacement of about 2mm (Fig. 13). It is notable that the station EOUT recorded motions different from other stations; this may be attributable to the fact that the

EOUT station is located at a higher elevation (1677.85m) relative to the other stations.

(2) The Western region

From 2005.4 and 2005.9, the stations in the west region all move in the southwest direction. Then they tend to form a pattern of motion that results in two zones of contraction. The first one is located in the area among MINE, LEWI and TOIY stations, and the second one is located between stations of SHNE and SLID (Fig. 15).

The stations also have displacements in the west to southwest direction during 2006.30 to 2006.80, which also results in two clear contractional belts. The first one is located between the centers of SHNE-GARL and SLID-USPA and the second one is located in the area of MINE, TOIY and BAMO (Fig. 16).

Notably, anomaly activities are observed for the station of MINE, with average distance of displacement much higher than the other stations to the west (highest 5.2mm).

Compared to the east stations, the stations in the west region are not moving with as a clear coherent pattern, but rather show more variability with respect to one another (resulting in the zones of contraction).

The signals from RUBY and ELOK are weak, but they are basically moving in the same manner as GOSH. The stations of EGAN and FOOT generally move in opposite directions. We thus divide the west and east regions according to the locations of these three stations.

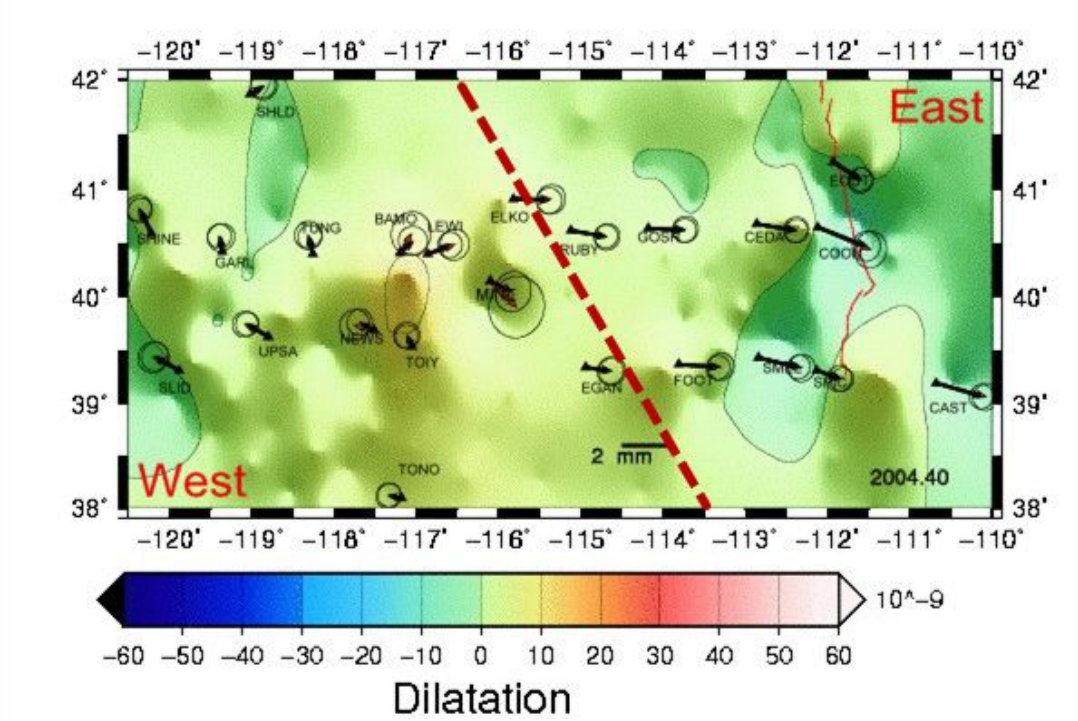

Fig. 9 Time-depend displacement and strain field in 2004.40. In the eastern part, the stations were moving towards east. Error ellipses are 95% confidence.

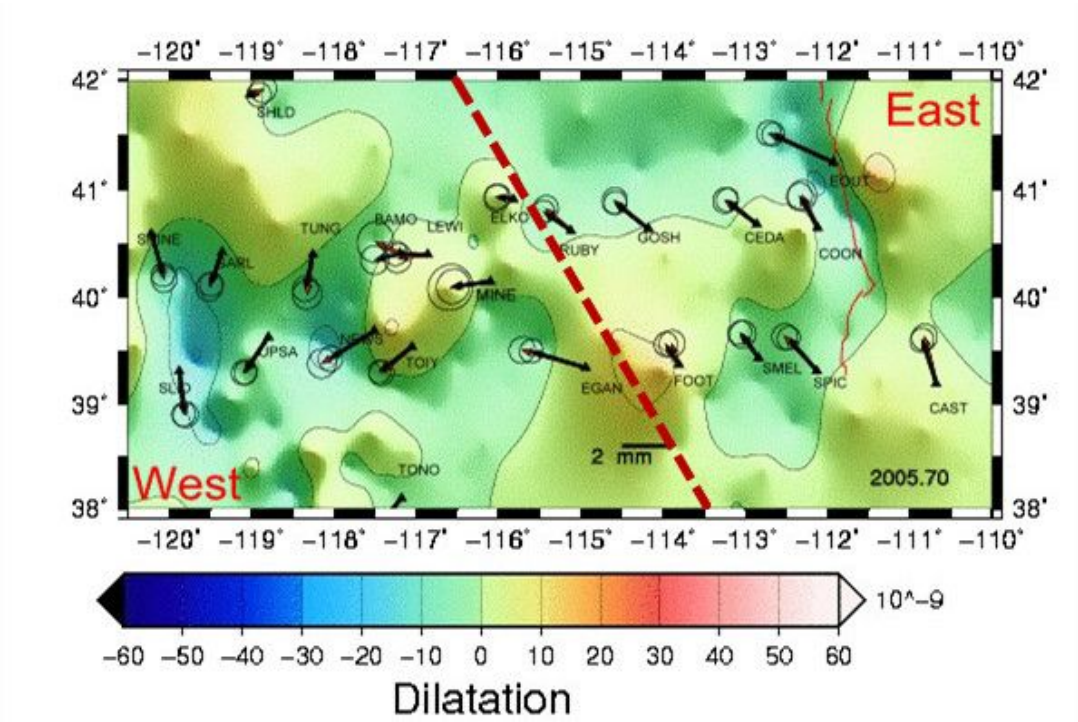

Fig. 10 Time-depend displacement and strain field in 2005.70. The stations were moving towards southeast. Error ellipses are 95% confidence.

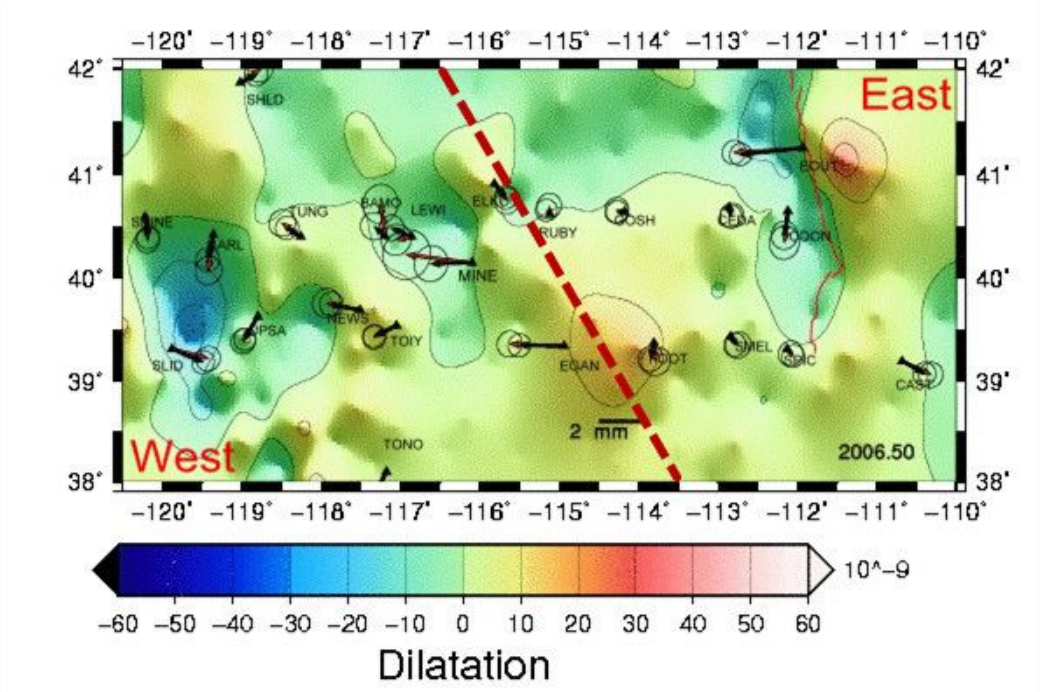

Fig. 11 Time-depend displacement and strain field in 2006.50. The signals of the displacements stations were small and the stations were in a quiet status. Error ellipses are 95% confidence.

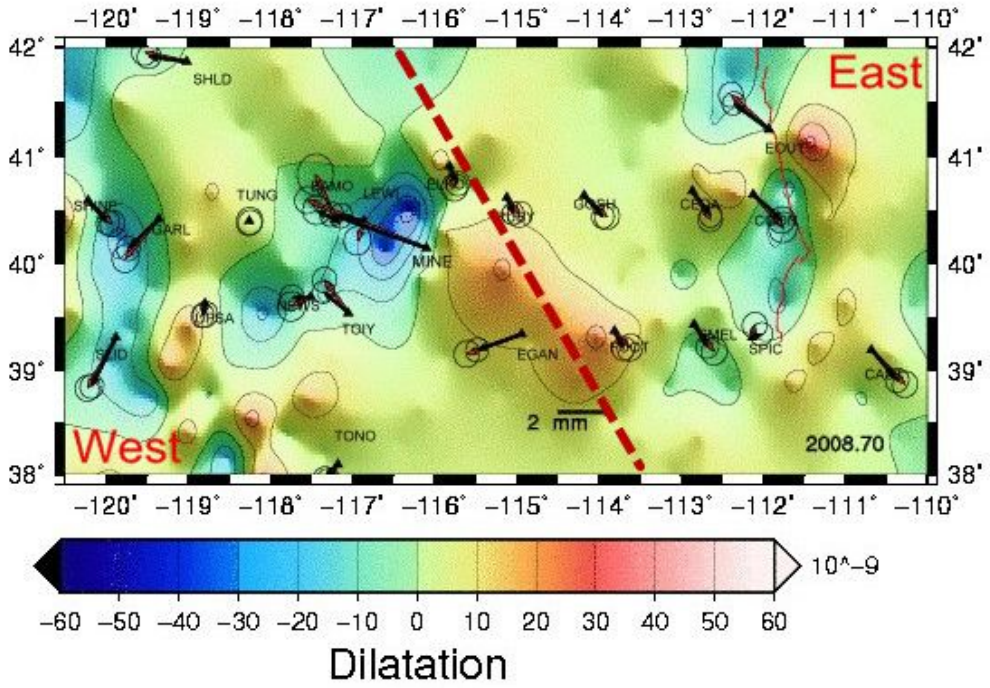

Fig. 12 Time-depend displacement and strain field in 2008.70. The stations were moving towards southeast. Error ellipses are 95% confidence.

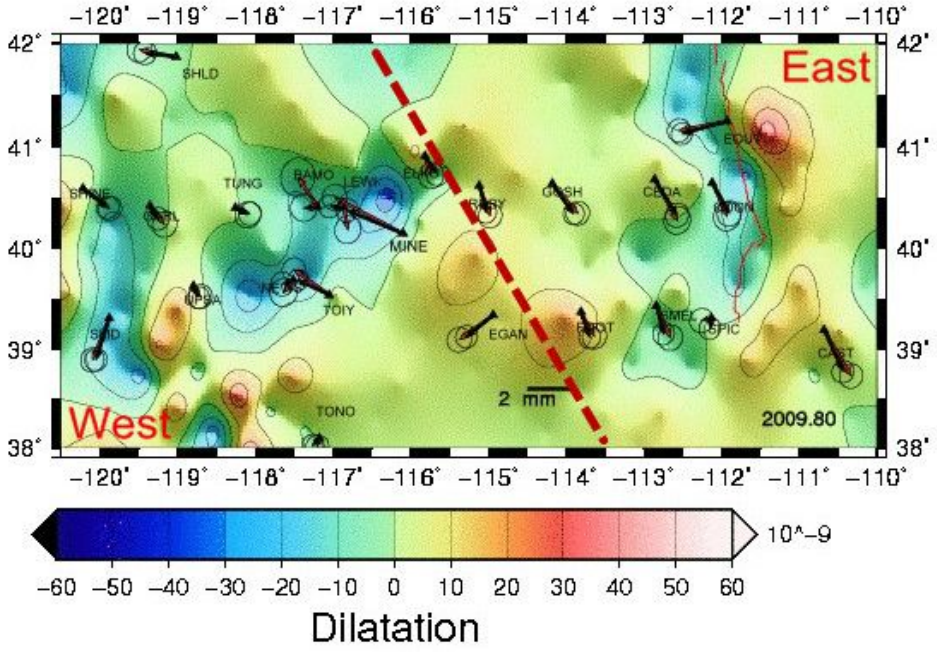

Fig. 13 Time-depend displacement and strain field in 2009.80. The stations were moving towards southeast. Error ellipses are 95% confidence.

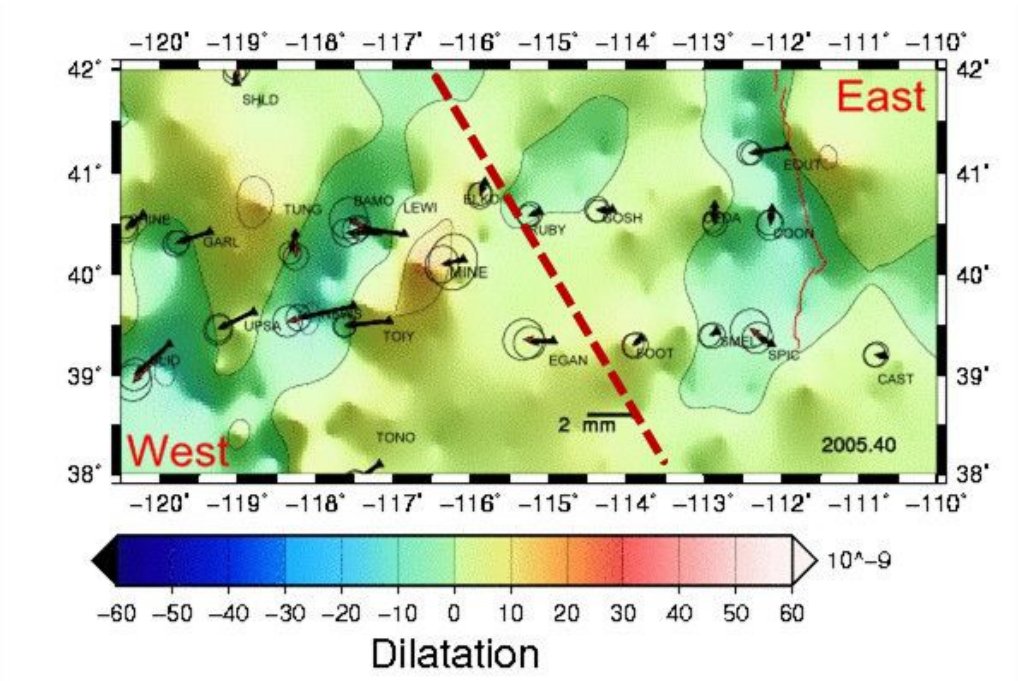

Fig. 14 At 2005.40, the stations in the western part of Great Basin were moving towards west. Error ellipses are 95% confidence.

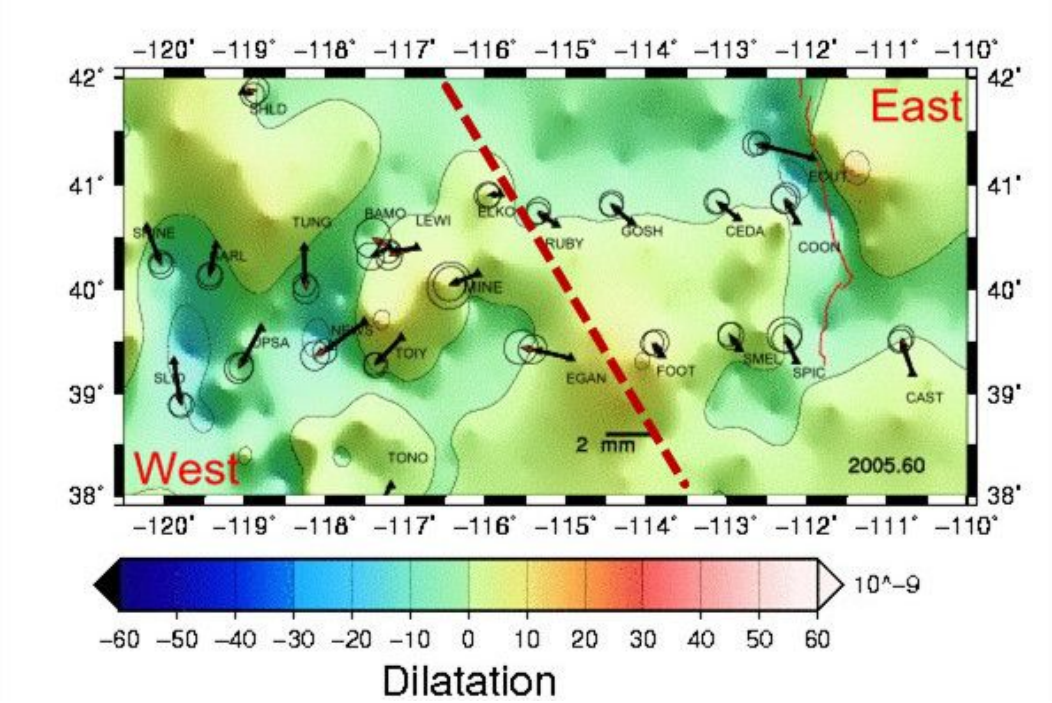

Fig. 15 At 2005.6 0, the movements of the stations tended to made two contractions. The first one located at the area among MINE, LEWI and TOIY stations and the second one located between stations of SHNE and SLID. Error ellipses are 95% confidence.

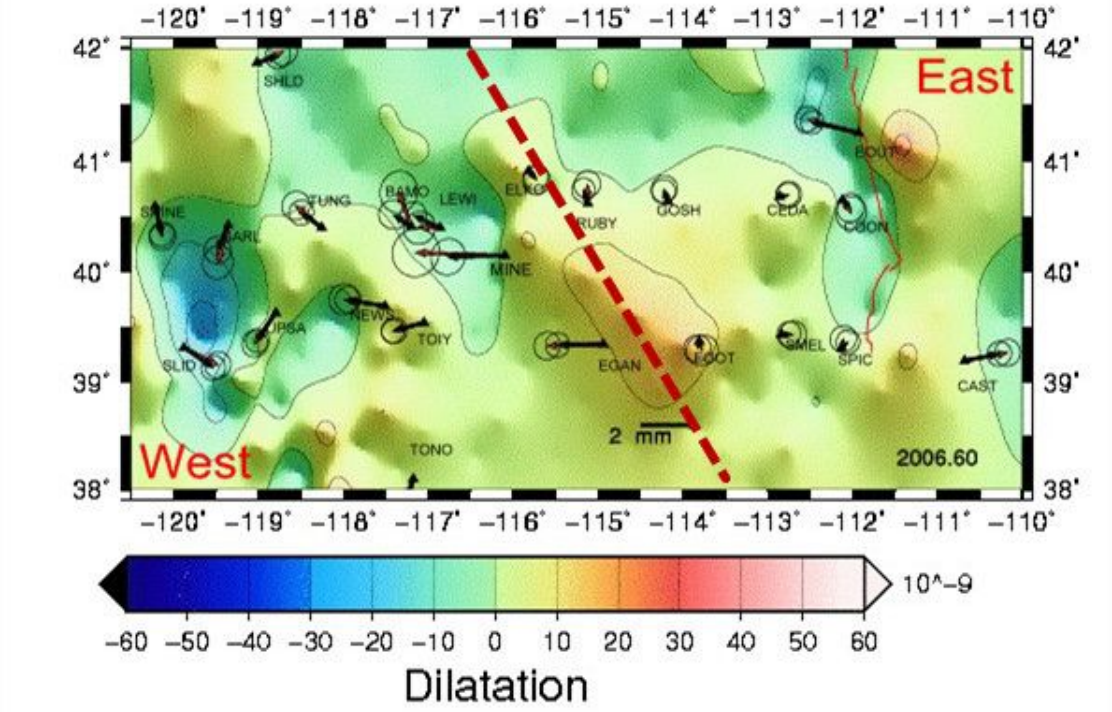

Fig. 16 At 2006.60, the movements of the stations tended to made two contractions. The first one located between the centers of SHNE-GARL and SLID-USPA and the second on located in the area of MINE, TOIY and BAMO. Error ellipses are 95% confidence.

Discussion

(1) A lithospheric drip beneath Great Basin

In the lithospheric drip model by West *et al*. [2009], the location of the drip, or fast mantle anomaly, is approximately at the center of the line we draw to separate the eastern and western part of the Great Basin (Fig. 17).

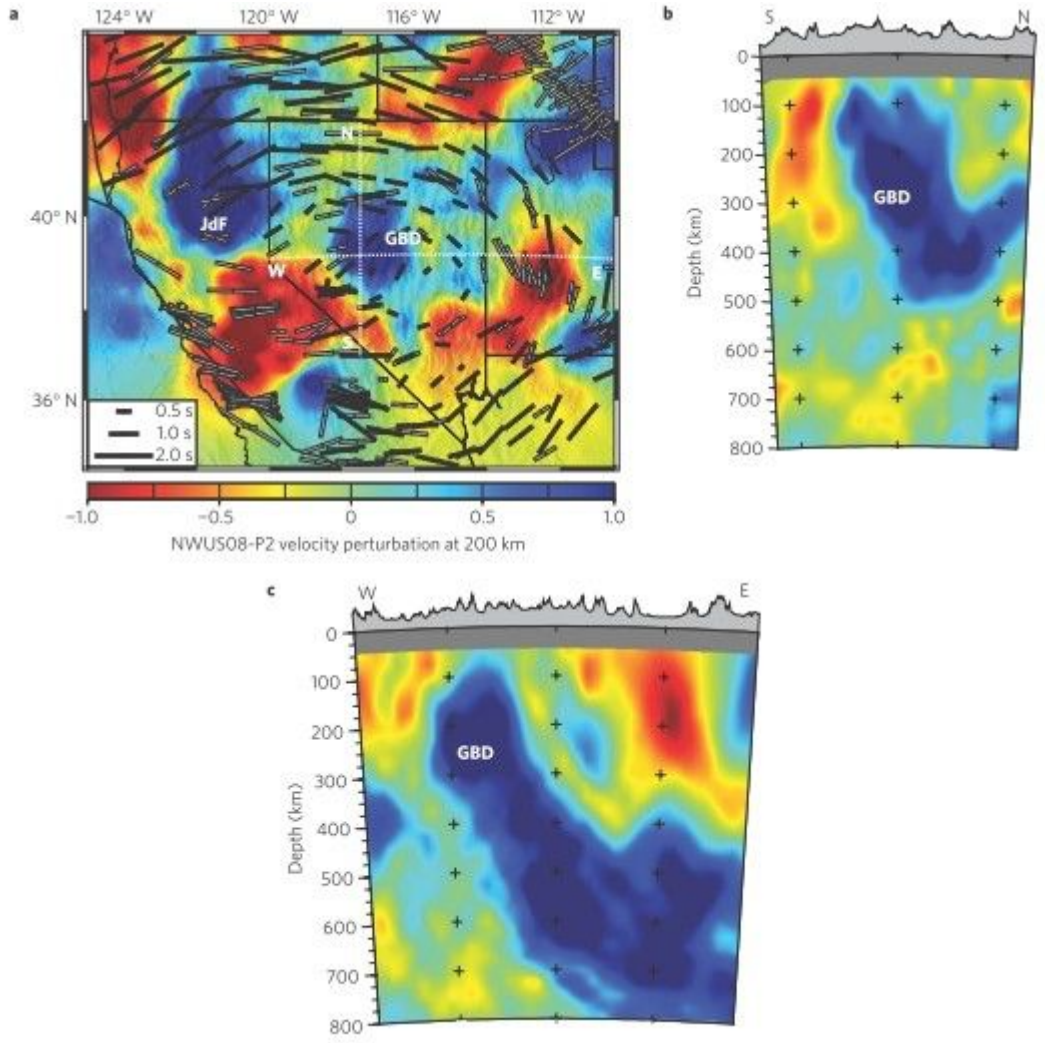

Fig. 17 A clear evidence of the drip with increased seismic velocities, and through the comparison of the location of a, b, c, we know the location of the drip [West *et al*., 2009].

The cartoon in Fig.18 shows a mantle flow field associated with this drip, which produces tractions that act on the base of the lithosphere and influence crustal strains.

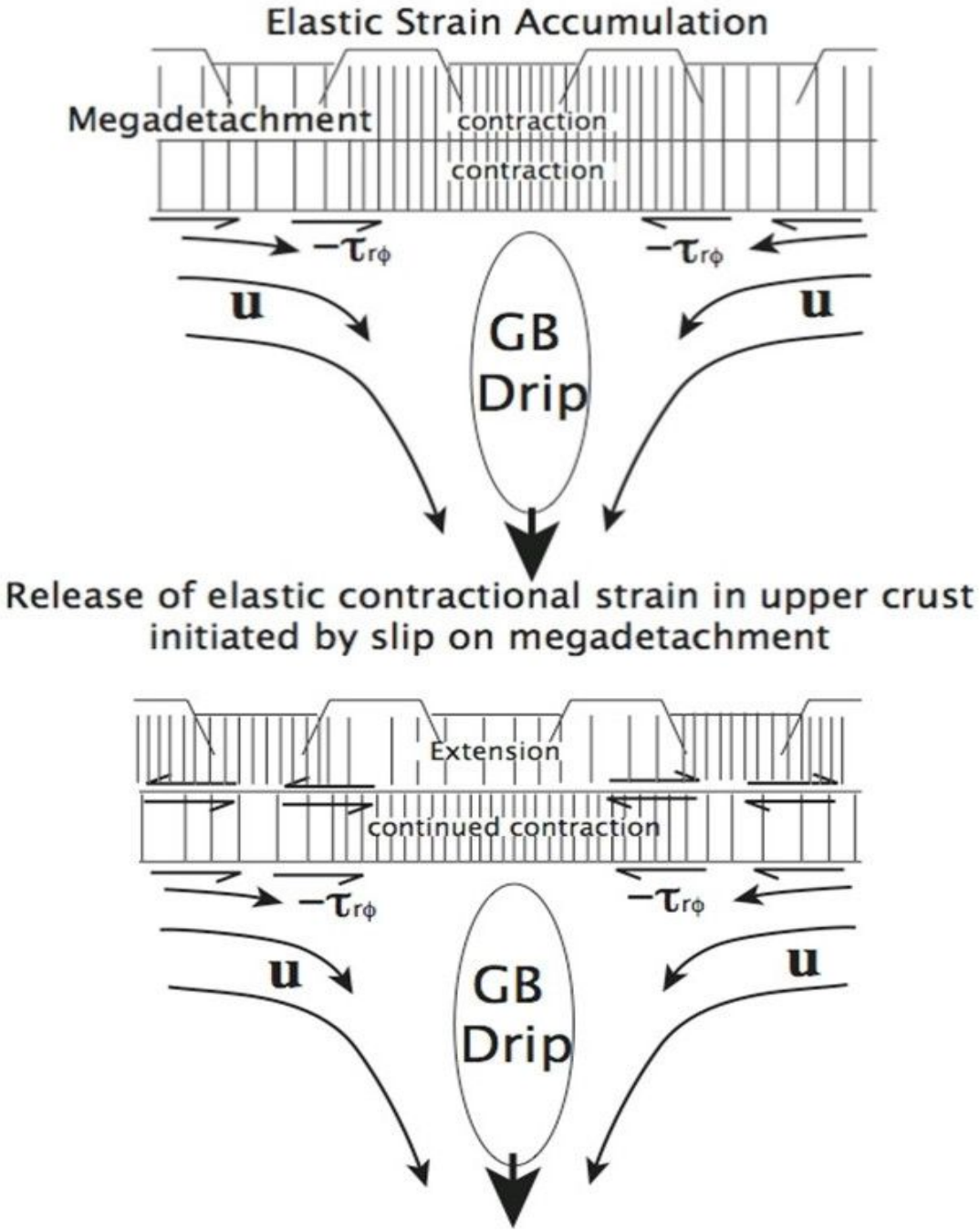

Fig. 18 A brief cartoon of Great Basin drip [W. E. Holt *et al*.in preparation]].

That is, with the sinking of the drip, stresses are generated at the bottom of the lower crust, and converge approximately in the area above the drip. This process produces stress to drive the lower crust and upper crust to contract in elastic strain. The elastic strain accumulation is

periodically relieved via slip along portions of the megadetachment. This periodic slip may then result in the transient motions observed at the surface GPS stations.

In the results presented above, the behavior of the eastern region of Great Basin may be in accord with this hypothesis. Periodic movement to the east may correspond with slip on the megadetachment, while the periods in between the pulses of eastward motion correspond to strain accumulation during the time that the megadetachment is locked. While the movement of stations in western region is more complicated, and the stations do not in general move as an entire body, the general region of contraction may also be consistent with the drip hypothesis. That is, the zone of crustal contraction lies above and slightly west of the Great Basin drip.

(2) Toroidal mantle flow through the western U.S. slab window

In the model set up by Zandt *et al*., toroidal mantle flow goes through the western U.S. slab window. This anticlockwise rotation of upper mantle flow will also induce a shearing relationship (tractions) with the lithosphere. The tractions acting on the bottom of the lithosphere lead to elastic deformation strain. This model is similar to the "lithosphere drip" model, but would result in a different pattern of expected slip on the megadetachment (due to toroidal pattern of mantle flow). This expected pattern would involve a different sense of shear imposed on the northern and southern Great Basin. This is not observed in the crustal transient pattern. However, the southeast motion of the eastern stations during the time periods of 2008.40 to 2009.00, and from 2009.50 to 2011.00 are consistent with slip on the megadetachment associated with the sense of shear direction in the toroidal flow model predicted beneath this area.

(3) Possible movement along an active megadetachment

The movement of the stations in eastern part of the Great Basin has a resemblance to Wernicke *et al*.'s hypothesis of a single megadetachment. However, the division of an eastern and western Great Basin is inconsistent with a single megadetachment acting in one entire phase of slip. The separate behaviors would require a pinning of the detachment in the central region in order to explain the separate behaviors in the east and west. Furthermore, the zones of contraction on the western side would require complicated variations in slip on the megadetachment beneath that area.

(4) The influence of variable hydrologic loading

In Heki's work, the movements of the GPS transients are towards the areas where there are loads of heavy snow pack. This is reasonable because the loading of snow will make a deformation that shows up as the surrounding stations moving towards the load (Fig. 19).

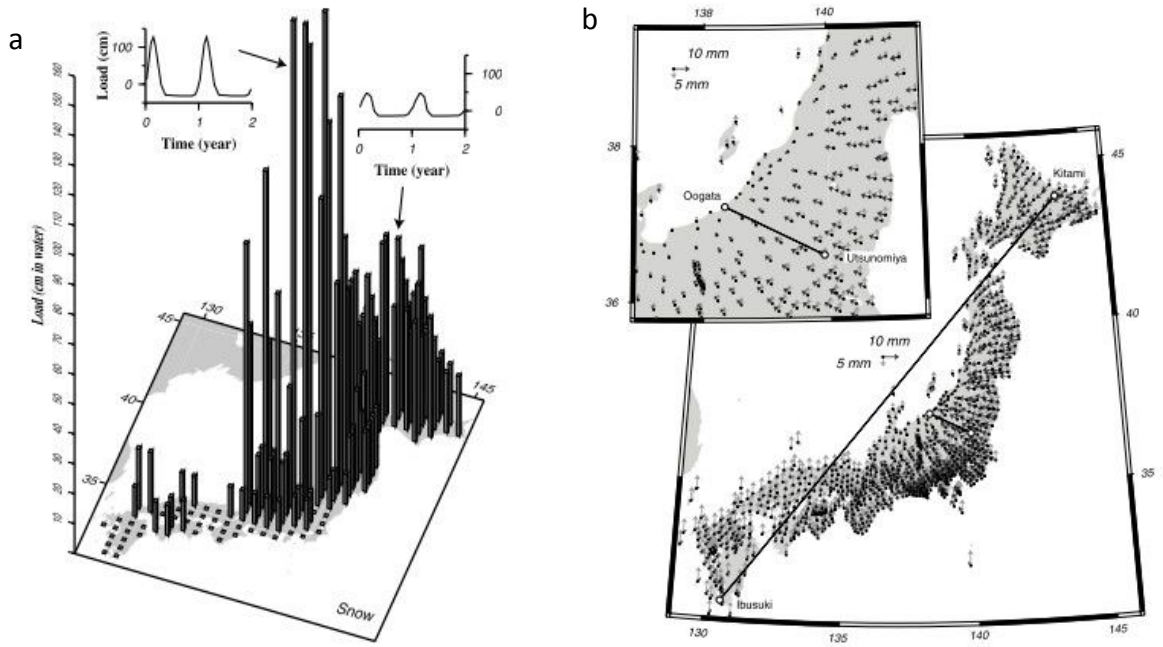

Fig. 19 (a) Differences between the maximum and the minimum value of snow loading in different areas in Japan. (b) Seasonal displacement in Japan. From these figures , the movement of the stations are towards the heaviest snow-loading areas. [G. Heki, 2013]

In the result of this thesis, during 2004.20 to 2006.30, the movements of the stations do have some regular pattern. During the late winter to early spring of 2004 to 2006, especially in 2004.40 and 2005.30 , the stations in the eastern part show a tendency to move to the east. In 2006.20 the direction is towards Southeast. But after 2006, the signals were either comparatively small or show no regularity of movement in correlation with seasons. In this way, the displacements of the first three years seem to show the seasonal influence that may be associated with snow loading in the Rockies. But the movements become more complicated after that. In western part, the movements of the stations are too irregular such that no clear seasonal signals exist.

To look further into how the snow loading influences the geodetic characteristics in this area, an analysis of the actual snow loading history is needed. Both of the quantity and distribution of snow loading details are required to build up this model.

Discussion and Conclusions

In conclusion, the drip model by West *et al*. [2009] and the snow loading hypothesis are the best ways to explain the displacement anomalies obtained in this thesis. The drip model is more consistent with geodetic evidence. This model is consistent with the divergence of displacement between the eastern and western parts of Great Basin. However, a megadetachment should exist in this situation to explain the back and forth movement of the displacements, and the contraction belts in the western part of Great Basin need to be investigated further.

The snow loading model can possibly explain the roughly east-west oscillation of displacements in the first three years (2004 – 2006). This hypothesis calls for more detailed information for further investigation.

1. A model of quantity of snow loading in the Rockies and the distribution of this loading should be investigated in detail.

2. The expected elastic response (expected wavelength of response and amplitude) of this snow loading needs to be addressed [Farrell, 1972] and compared with observation.

Reference

B. Wernicke *et al*., Active megadetachment beneath the western United States, *Journal of Geophysical Research*, 2008, **113 (**B11409**)**, 1-26.

B. Wernicke *et al*., Detecting large-scale intracontinental slow-slip events (SSES) using geodograms, *SRL*, 2010, **81(5)**, 694-698.

B. Wernicke, Low-angle normal faults in the Basin and Range province: Nappe tectonics in an extending orogen, *Nature*, 1981, **291**, 645-648.

G. Blewitt *et al*., Geodetic observation of contemporary deformation in the northern Walker Lane: 1. Semipermanent GPS strategy, *The Geological Society of America Special Paper*, 2009, **447**, 1-15.

G. Zandt *et al.*, Toroidal mantle flow through the western U.S. slab window, *Geology*, 2008, **36**(4), 259-298.

J. D. West *et al*, Vertical mantle flow associated with a lithospheric drip beneath the Great Basin, *Nature Geosciences*, 2009, **2**, 439-444.

K. Heki, Dense GPS Array as a New Sensor of seasonal Changes of Surface Loads, *The State of the Planet Frontiers and Challenges in Geophysics*, 2013.

M. Ohtake *et al*., Seasonality of great earthquake occurrence at the northwestern margin of the Philippine Sea Plate, *Pure Appl. Geophys*., 1999, **155**, 689–700.

P. Elosegui *et al*, Measurement of crustal loading using GPS near Great Salt Lake, Utah, *GRL*, 2003, **30**, 1111–1114.

R. McCaffrey *et al*., Fault locking, block rotation and crustal deformation in the Pacific Northwest, Geophysical Journal International, **2007**, 169, 1315-1340.

Severinghaus et al, Cenozoic geometry and thermal state of the subducting slabs beneath North America, Wernicke, B.P., ed., Basin and Range extensional tectonics near the latitude of Las Vegas, Nevada: Geological Society of America Memoir **176**, 1–22.

W. E. Holt et al, Toward a continuous monitoring of the horizontal displacement gradient tensor field in southern California using cGPS observations from Plate Boundary Observatory (PBO), SRL, 2013, **84**, 455-467.

W. E. Farrell, Deformation of the Earth by Surface Loads, *Reviews of Geophysics And Space Physics*, 1972, **10: 3**, 761-797.

Williams *et al.*, Unlocking the secrets of the north American continent: an EarthScope science Plan for 2010-2020, 2010, 8.

W. R. Dickinson *et al*, Geometry of subducted slabs related to the San Andreas transform, *Journal of Geology*, 1979, **87**, 609-627.

Appendix

For all the time-series, a and c are in the direction of north-south displace components, while b and d are in the direction of east-west displace components. In a, b, the blue dots are raw data, and the red curve fits the blue dots, annual and semiannual terms; In c, d the red curve fit to the yellow dots (which is also the raw data), 0.15 year moving average (centered) fit to residual time series (annual and semiannual terms removed), and red line, the fourth-order polynomial fit to the cleaned time series.

1, Time series of LEWI.

a

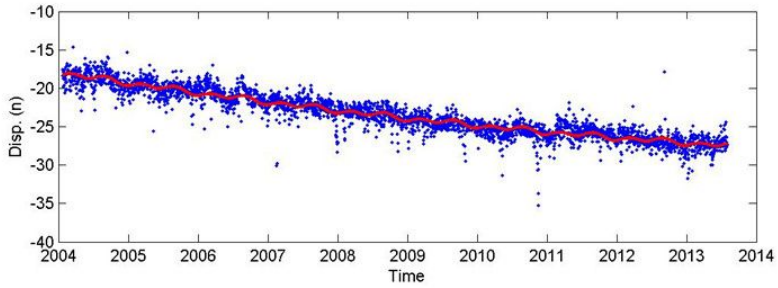
Disp. (n)
Time
-10
-15
-20
-25
-30
-35
-40
2004
2005
2006
2007
2008
2009
2010
2011
2012
2013
2014

b

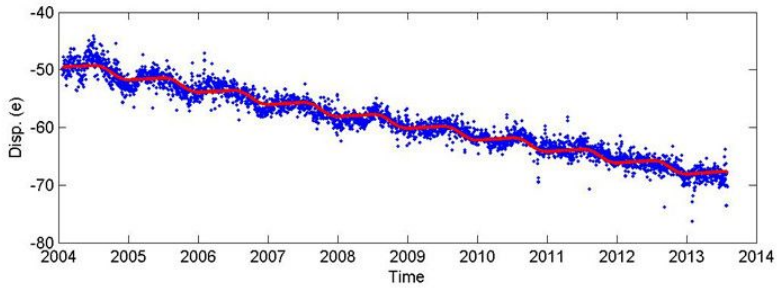
Disp. (e)
Time
-40
-50
-60
-70
-80
2004
2005
2006
2007
2008
2009
2010
2011
2012
2013
2014

c

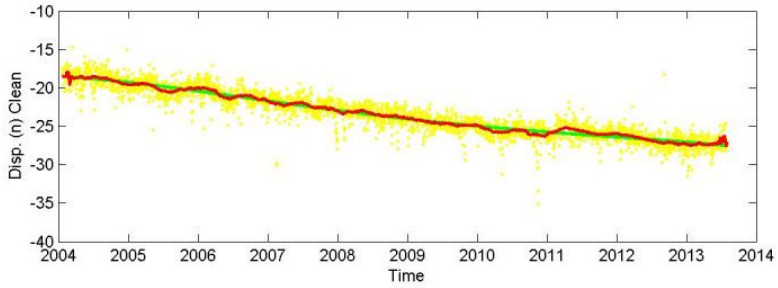
Disp. (n) Clean
Time
-10
-15
-20
-25
-30
-35
-40
2004
2005
2006
2007
2008
2009
2010
2011
2012
2013
2014

d

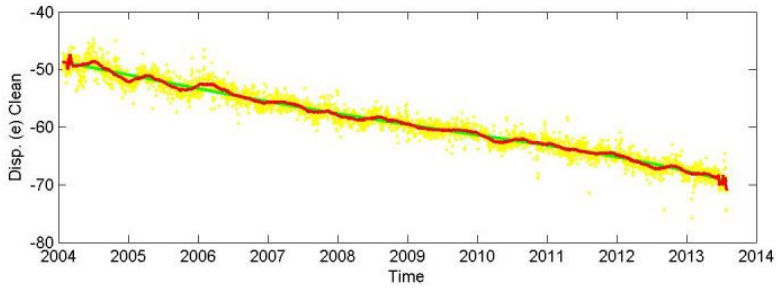
Disp. (e) Clean
Time
-40
-50
-60
-70
-80
2004
2005
2006
2007
2008
2009
2010
2011
2012
2013
2014

2. Time series of GARL.

a

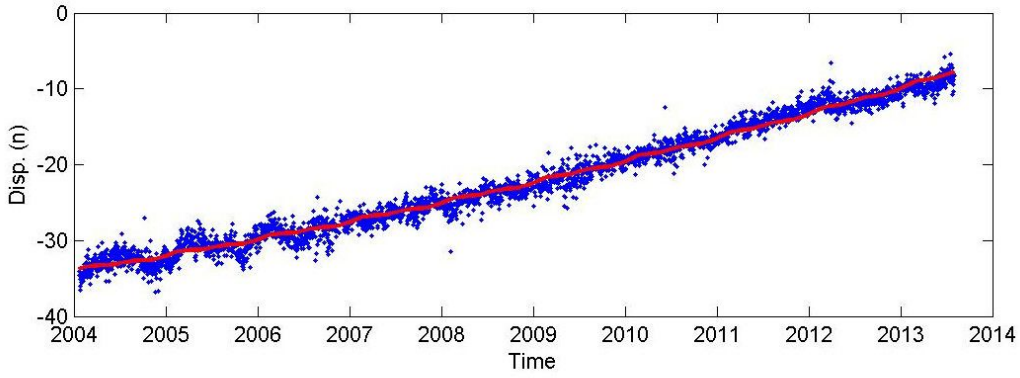

b

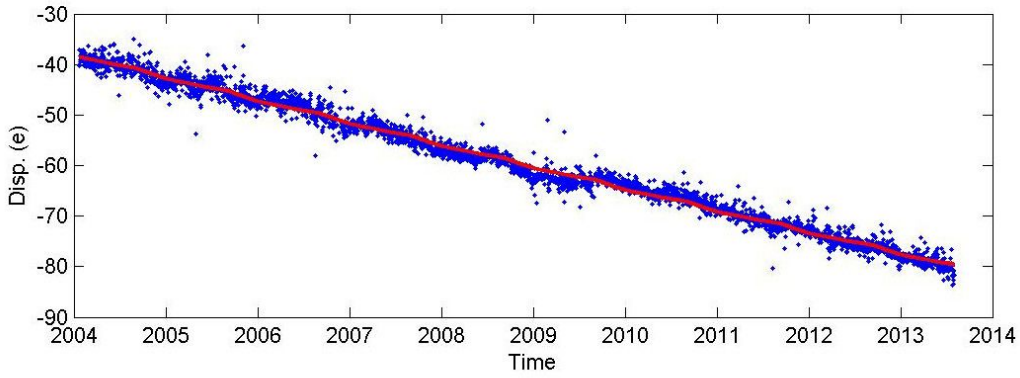

c

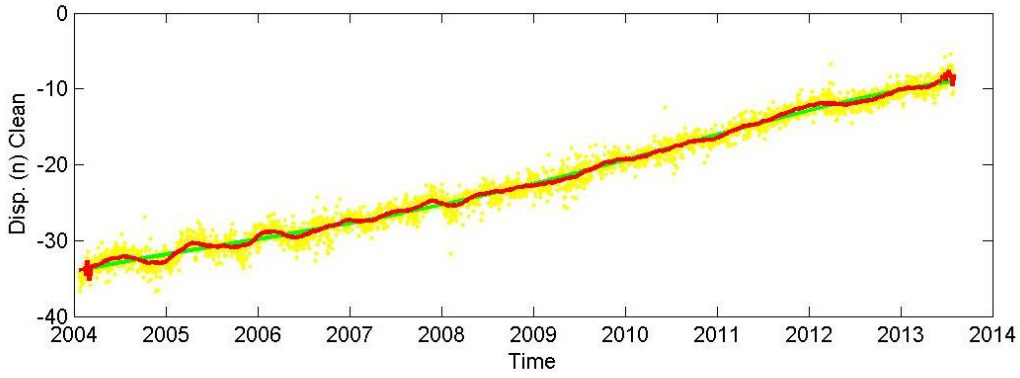

d

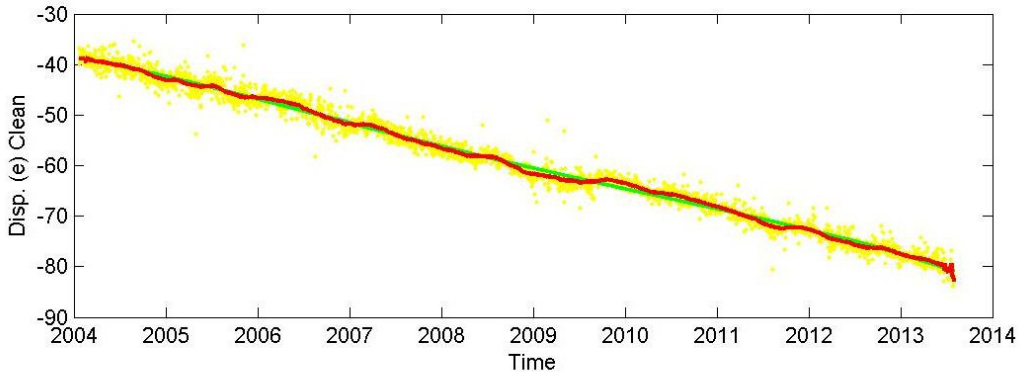

3. Time series of CEDA.

a

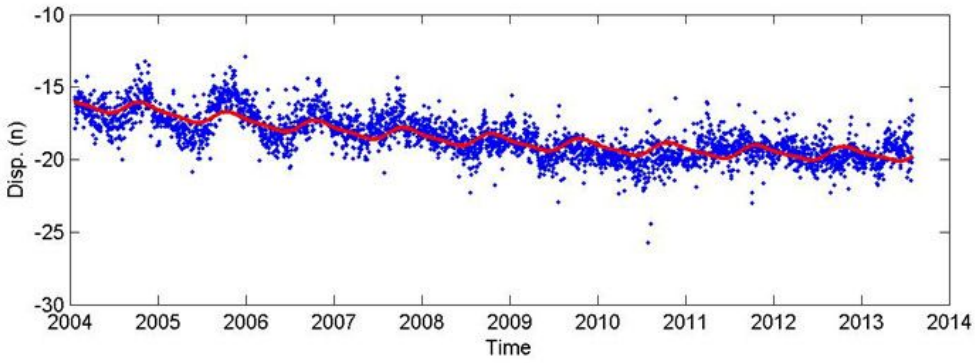

b

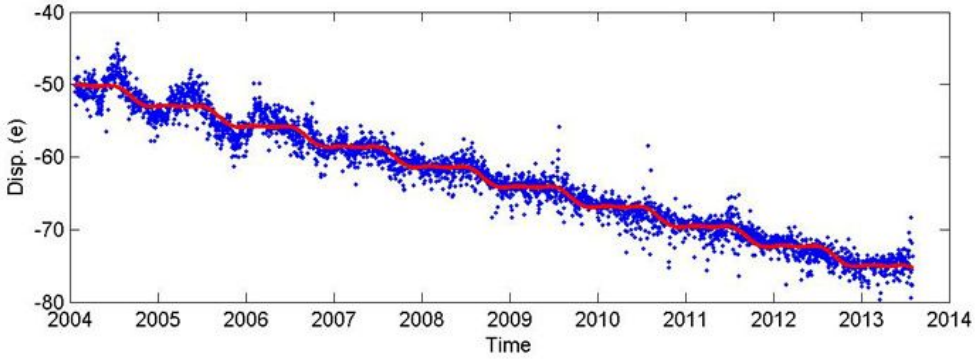

c

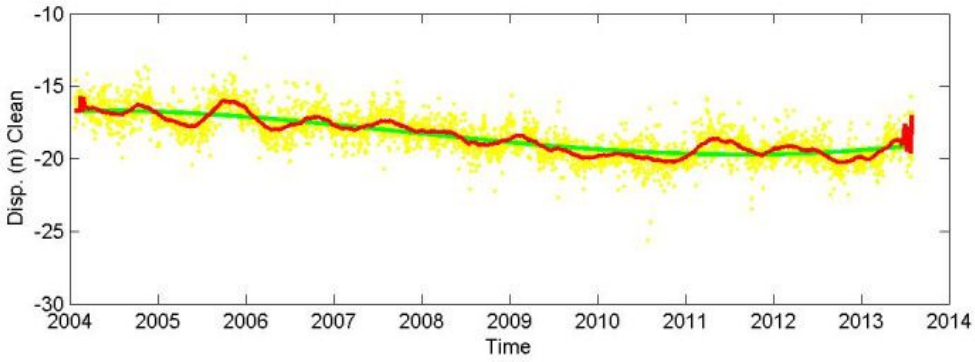

d